Unique Chemical Reactivities of Nanocrystalline Metal Oxides toward Hydrogen Sulfide

Corrie L. Carnes and Kenneth J. Klabunde*

Department of Chemistry, Kansas State University, Manhattan, Kansas 66506

Received November 2, 2001. Revised Manuscript Received January 23, 2002

Nanocrystalline metal oxides prepared through sol−gel or aerogel syntheses were allowed to react with hydrogen sulfide and compared with microcrystalline commercially available metal oxides. The nanocrystalline metal oxides were found to be considerably more reactive than the commercial samples, as a result of their higher surface areas as well as higher intrinsic reactivities. In some cases, nearly stoichiometric solid−gas reactions took place at selected elevated temperatures, and the oxides exhibited a general reactivity trend of CaO > ZnO > Al_2O_3 > MgO. At lower temperatures (25−100 °C), the trend was ZnO > CaO > Al_2O_3 ≈ MgO. Core/shell particles, where a thin layer of Fe_2O_3 was deposited on nanocrystalline CaO, yielded the best results, thus demonstrating another example of transition metal oxide catalysis in solid−gas reactions.

I. Introduction

A common impurity in chemical feedstocks, natural gas streams, and crude oil streams is hydrogen sulfide (H_2S), which is very toxic, hazardous, and corrosive.[1,2] Many methods have been studied for the removal H_2S from commercial processes. The most common methods for desulfurization are catalysis and adsorption. Catalysis, however, only deals with the H_2S once it has been removed, and our aim is to study the removal of H_2S by adsorption.

Selective removal of H_2S via reaction with or adsorption onto metal oxides is a well-known method. Of all metal oxides studied, ZnO is one of the most commonly used. In 1995, Davidson, Lawrie, and Sohail published results on the adsorption of H_2S onto 300−710-μm particles of ZnO, studied in flow reactors with low concentrations of H_2S and H_2O present.[3] These reactions were carried out at ambient conditions (25−45 °C), and about 40% conversion of H_2S was observed. However, the reactions were not carried out to saturation, so the total percentage of ZnO converted to ZnS was not reported. Another paper reporting on ZnO by Sasaoka, Hirano, Kasaoka, and Sakato discussed the effects of the presence of CO, CO_2, and H_2O on the reaction.[4] The authors found that CO inhibited the reaction by adsorbing onto the active sites, and H_2O was found to inhibit the reaction by causing a back reaction with the ZnS to form H_2S and ZnO. In a study by Rodriguez and Maiti, the adsorption of H_2S on MgO was compared to that on ZnO and the reaction of ZnO toward H_2S was found to be much more efficient.[5] Next, they compared their results to previously studied Al_2O_3, Cr_2O_3, Cr_3O_4, and Cu_2O and found a trend between the band gap energy and chemical reactivity (availability to adsorb H_2S). It was found that the lower the band gap energy, the more H_2S was adsorbed.

Overall, many techniques have been studied for the removal of H_2S, but few have studied the chemical reactivity differences of bulk metal oxides compared with ultrafine metal oxides. This will be the focus of this paper, and the reactivity of various nanoparticle metal oxides with H_2S compared with that of bulk metal oxides will be discussed. The catalytic effect of Fe_2O_3 will also be described.

In this paper, several metal oxides were allowed to react with H_2S, and the desired products are the corresponding metal sulfides and water. Table 1 shows the standard heats of formation of the compounds studied, and it can be seen that some of these reactions are thermodynamically favorable (eqs 1−4).[6] Thermodynamics can predict that the reactivities of the metal oxides will be as follows, from most reactive to least: ZnO, CaO, MgO, with Al_2O_3 not being reported. However, it will be seen how surface area, crystallite size, and intrinsic crystallite reactivity can play a role.

II. Experimental Section

A. Preparation and Characterization of Metal Oxides. All of the nanocrystalline metal oxides have been previously discussed in detail.[7−16] The metal oxides studied include nanocrystalline (NC) Al_2O_3, conventionally prepared (CP) and

(1) Capone, M., Kroschwitz, J. K., Howe-Grant, M., Eds. *Encyclopedia of Chemical Technology*; Wiley: New York, 1997; Vol. 23, p 432.
(2) Berkow, R., Ed. *The Merck Manual of Diagnosis and Therapy*, 16th ed.; Merck Research Laboratories: Rahway, NJ, 1992; p 2691.
(3) Davidson, J. M.; Lawrie, C. H.; Sohail, K. *Ind. Eng. Chem. Res.* **1995**, *34*, 2981.
(4) Sasaoka, E.; Hirano, S.; Kasasoka, S.; Sakata, Y. *Energy Fuels* **1994**, *8*, 1100.
(5) Rodriguez, J. A.; Maiti, A. *J. Phys. Chem. B* **2000**, *104* (15), 3630.
(6) Barin, I.; Knacke, O. *Thermochemical Properties of Inorganic Substances*; Springer-Verlag: Berlin, 1973.
(7) Klabunde, K. J.; Stark, J.; Koper, O.; Mohs, C.; Park, D. G.; Decker, S.; Jiang, Y.; Lagadic, I.; Zhang, D. *J. Phys. Chem.* **1996**, *100* (30), 12142.
(8) Carnes, C. L.; Klabunde, K. J. *Langmuir* **2000**, 16, 8, 3764.
(9) Carnes, C. L.; Stipp, J.; Klabunde, K. J. *Langmuir*, in press.
(10) Carnes, C. L.; Klabunde, K. J. *Chem. Mater.*, submitted.
(11) Koper, O. B.; Lagadic, I.; Volodin, A.; Klabunde, K. J. *Chem. Mater.* **1997**, *9*, 2468.

10.1021/cm011588r CCC: $22.00
Published on Web 03/09/2002

Table 1. Standard Heats of Formation

compound	$\Delta H_f°$ (kJ/mol)	compound	$\Delta H_f°$ (kJ/mol)
Al_2O_3	−1632	Al_2S_3	NR[a]
CaO	−634	CaS	−476
MgO	−583	MgS	−347
ZnO	−339	ZnS	−202

[1] $Al_2O_3 + 3H_2S \rightarrow Al_2S_3 + 3H_2O$ $\Delta H_{rxn}° = NR$[a]
[2] $CaO + H_2S \rightarrow CaS + H_2O$ $\Delta H_{rxn}° = -63.5$ kJ/mol
[3] $MgO + H_2S \rightarrow MgS + H_2O$ $\Delta H_{rxn}° = 14.5$ kJ/mol
[4] $ZnO + H_2S \rightarrow ZnS + H_2O$ $\Delta H_{rxn}° = -84.5$ kJ/mol

[a] Not reported.

aerogel-prepared (AP) MgO, AP- and CP-CaO, NC-ZnO, and all of their commercial (CM) counterparts.

B. GC Studies. The reactions between H_2S and the metal oxides were carried out to determine the best conditions for destructive adsorption. The reactions were conducted in a U-tube that was connected to a gas chromatograph (GOW-MAC gas chromatograph series 580).[11] The U-tube was made of Pyrex and connected between the injector port and the column (Alltech Porapak Q). A metal oxide sample (0.100 g) was placed in the U-tube between two small plugs of aluminum silicate wool. The reactor was then heated to the desired temperature. Pulses of 1 mL of H_2S gas were made through the injector port (110 °C) every 12 min. Any H_2O coming off the sample or H_2S that was not destroyed was then sent via helium (30 cm^3/min) through the column (100 °C) to be separated. They were then detected by a thermal conductivity detector (120 °C), and their peak areas were recorded. Injections of H_2S were made until the metal oxide beds were exhausted.

(1) Thermal Decomposition. Blank reactions with just the aluminum silicate in the reaction tube and no metal oxide present were carried out. This was done to record any H_2S decomposition due to the reaction temperature and any adsorption by or reaction with the aluminum silicate wool. These reactions would then serve as the background reactions to be subtracted from actual reactions involving metal oxides.

(2) Reaction Decomposition. To study the decomposition of H_2S on various metal oxides, 0.100 g amounts of the metal oxide were placed into the reactor, and the reaction was carried out at the desired temperature found for each metal oxide. Nanocrystalline Al_2O_3, MgO, CaO, and ZnO were then individually studied and compared to commercial brands. The reactivities of the samples were compared on a per weight basis.

After the reactions, the samples were also studied by XRD on a Scintag XDS 2000 spectrometer. Cu Kα radiation was the light source used, with an applied voltage of 40 KV and a current of 40 mA. The angle (2θ) ranged from 20° to 85° at a speed of 2°/min. The crystallite size was then calculated from the XRD spectra using the Scherrer equation.

III. Results

A. Preparation and Characterization of Metal Oxides. The NC-ZnO and NC-Al_2O_3 samples and the nanocrystalline CaO and MgO samples known as conventionally prepared (CP) and aerogel-prepared (AP) were prepared as described earlier, without additional treatment.[7−10] The CaO and MgO samples were previously found to have an enhanced reactivity with an iron oxide coating.[12−14] Thus, in addition to the NC-ZnO and NC-Al_2O_3 samples, CP-CaO, AP-CaO, CP-MgO, AP-MgO, [Fe_2O_3]CP-CaO, [Fe_2O_3]AP-CaO, [Fe_2O_3]CP-MgO, and [Fe_2O_3]AP-MgO samples were also studied. All CaO and MgO samples with and without iron oxide coatings have been previously prepared and characterized in detail.[7,12−14] Commercial (CM) samples include Fisher ZnO (CM-1-ZnO), Nanophase Technologies ZnO (CM-2-ZnO), Baker Analytical Al_2O_3 (CM-Al_2O_3), Aldrich MgO (CM-MgO), and Fisher CaO (CM-CaO). Because a detailed characterization has already been discussed, only a brief summary is provided in this section to compare the five oxides studied. Table 2 shows the surface area, obtained via BET, and crystallite size, obtained via XRD, of the NC powder samples and their corresponding CM powder samples. Along with the enthalpies discussed earlier, this table provides important information that will play a significant role in the level of reactivities. Surface areas ranging from 2 to 800 m^2/g and crystallite sizes ranging from <2 to 93 nm can have a tremendous effect on how reactive a sample proves to be.

Table 2. Sample Characteristics

sample	surface area (m^2/g)	crystallite size (nm)
NC-Al_2O_3	800	<2
CM-Al_2O_3	100	19
AP-MgO	452	4
CP-MgO	170	7
[Fe_2O_3]AP-MgO	427	4.5
[Fe_2O_3]CP-MgO	156	7
CM-MgO	19	87
AP-CaO	122	7
CP-CaO	100	15
[Fe_2O_3]AP-CaO	114	7
[Fe_2O_3]CP-CaO	93	15
CM-CaO	2	93
NC-ZnO	130	4
CM-1-ZnO	3.9	44
CM-2-ZnO	20	33

B. GC Studies. *(1) Thermal Decomposition.* To record any H_2S decomposition due to temperature or adsorption/reaction with the aluminum silicate wool, blank reactions were carried out. At temperatures from room temperature to 500 °C, no decomposition or reaction of H_2S was observed.

(2) Dependence on Temperature. As expected, as the temperature was raised from room temperature, the reaction efficiency increased. It was found that this trend continued until the temperatures were sufficient to sinter the metal oxide, which resulted in a lowering of the reaction efficiencies. Because this effect is dependent on the crystal sintering temperature, each metal oxide behaved differently. Thus, a study was conducted to find the optimum reaction temperature for each metal oxide. The breakthrough injection is defined here as the number of 1-mL injections that made before the first trace of excess H_2S is eluted from the bed of the adsorbent.

For aluminum oxide, calcium oxide, and magnesium oxide, it was observed that, although the CM samples were not very reactive, the NC samples continued to increase in reactivity up to 500 °C. This was chosen as the optimum temperature to study these samples not only for this reason, but also because it was found that going above 500 °C caused a loss in surface area, which

(12) Klabunde, K. J.; Khaleel, A.; Park, D. *High Temperature Mater. Sci.* **1995**, *33*, 99.
(13) Decker, S.; Klabunde, K. J. *J. Am. Chem. Soc.* **1996**, *118* (12), 465.
(14) Jiang, Y.; Decker, S.; Mohs, C.; Klabunde, K. J. *J. Catal.* **1998**, *180*, 24.
(15) Decker, S.; Lagadic, I.; Klabunde, K. J.; Michalowicz, A.; Moscovici, J. *Chem. Mater.* **1998**, *10*, 674.
(16) Moscovici, J.; Benzakour, M.; Decker, S.; Carnes, C.; Klabunde, K.; Michalowicz, A. *J. Synchrotron Rad.* **2001**, 8, 925.

Table 3. H_2S Reaction Characteristics

sample	breakthrough injection	saturation injection	temp (°C)	molar ratio (overall efficiency)	efficiency [(mol of H_2S)/(mol of oxide)]
CM-Al_2O_3	1	3	500	(1 mol of H_2S):(340 mol of Al_2O_3)	0.0030
NC-Al_2O_3	1	12	500	(1 mol of H_2S):(35 mol of Al_2O_3)	0.029
CM-MgO	1	2	500	(1 mol of H_2S):(2700 mol of MgO	0.0004
CP-MgO	1	2	500	(1 mol of H_2S):(240 mol of MgO)	0.0042
AP-MgO	1	2	500	(1 mol of H_2S):(190 mol of MgO)	0.0053
[Fe_2O_3]AP-MgO	1	5	500	(1 mol of H_2S):(70.2 mol of MgO)	0.014
[Fe_2O_3]CP-MgO	1	3	500	(1 mol of H_2S):(97 mol of MgO)	0.010
CM-CaO	71	5	500	(1 mol of H_2S):(5.2 mol of CaO)	0.19
CP-CaO	12	24	500	(1 mol of H_2S):(2.6 mol of CaO)	0.35
AP-CaO	16	28	500	(1 mol of H_2S):(2.1 mol of CaO)	0.47
[Fe_2O_3]AP-CaO	34	42	500	(1 mol of H_2S):(1.2 mol of CaO)	0.83
[Fe_2O_3]CP-CaO	24	34	500	(1 mol of H_2S):(1.7 mol of CaO)	0.59
CM-1-ZnO	2	3	250	(1 mol of H_2S):(32 mol of ZnO)	0.031
CM-2-ZnO	5	8	250	(1 mol of H_2S):(5.8 mol of ZnO)	0.17
NC-ZnO	10	18	250	(1 mol of H_2S):(2.4 mol of ZnO)	0.42

would hinder reactivity, and that thermal decomposition would occur at elevated temperatures. The zinc oxide samples were found to also be most reactive at 250 °C, and at higher temperatures, their reactivities decreased. Thus, the optimum temperature used for the zinc oxide samples was 250 °C.

(3) Destructive Adsorption of H_2S at Preset Temperature. Each of the metal oxide samples was then studied in more detail at the temperature found most favorable. The breakthrough injections, saturation injections, molar ratios, and reaction efficiencies are reported in Table 3. The reaction efficiencies are in terms of the number of moles of H_2S per mole of metal oxide.

It is clear from these results that the NC samples are much more reactive than the CM samples. CM-Al_2O_3 is not very reactive, with a breakthrough number of 1 and a saturation number of 3, whereas NC-Al_2O_3 has a breakthrough number of 1 and a saturation number of 12. The reaction efficiencies for the CM-Al_2O_3 and NC-Al_2O_3 are 0.0029 and 0.029, respectively.

Much like NC-Al_2O_3, the nanocrystalline MgO samples provide better reaction efficiencies than CM-MgO, with 2% [Fe_2O_3]AP-MgO being the most efficient. The experimental molar ratios are (1 mol of H_2S):(2700 mol of CM-MgO), (1 mol of H_2S):(240 mol of CP-MgO), (1 mol of H_2S):(190 mol of AP-MgO), (1 mol of H_2S):(70.2 mol of [Fe_2O_3]AP-MgO), (1 mol of H_2S):(97 mol of [Fe_2O_3]-CP-MgO), whereas the theoretical molar ratio is (1 mol of H_2S):(1 mol of MgO).

The nanocrystalline CaO also shows an increase in reactivity over CM-CaO. CM-CaO is reactive, with a breakthrough number of 7 and a saturation number of 15, whereas CP-CaO has a breakthrough number of 12 and a saturation number of 24, and AP-CaO has a breakthrough number of 16 and a saturation number of 28. The iron oxide-coated samples also show an increased reactivity, with [Fe_2O_3]AP-CaO having a breakthrough number of 34, a saturation number of 42, and a molar ratio of (1 mol of H_2S):(1.2 mol of CaO), which is very close to the 1:1 theoretical ratio. [Fe_2O_3]-CP-CaO had a breakthrough number of 24 and a saturation number of 34, with a molar ratio of (1 mol of H_2S):(1.7 mol of CaO). Figure 1 shows the percentage H_2S decomposition vs injection number. This graph shows that, whereas the CM-CaO quickly loses reactivity, the nanocrystalline CaO continues to destroy H_2S.

Last, NC-ZnO also shows an increase in reactivity over the CM-ZnO samples. CM-1-ZnO is one of the least

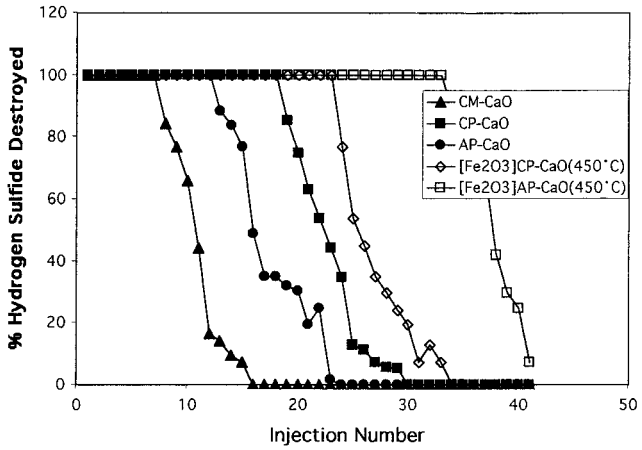

Figure 1. Percentage H_2S destroyed vs injection number for CaO at 500 °C.

reactive samples, having a breakthrough number of 2 and a saturation number of 3, whereas CM-2-ZnO sample has a breakthrough number of 5 and a saturation number of 8, and the NC-ZnO sample has a breakthrough number of 10 and a saturation number of 18. The reaction efficiencies for the CM-1-ZnO, CM-2-ZnO, and NC-ZnO are 0.0312, 0.172, and 0.417, respectively.

Next, the most reactive samples were studied at lower temperatures. Previous work was done at the optimum temperature for each oxide, that is, ZnO samples were allowed to react at 250 °C, whereas all others were allowed to react at 500 °C. Thus, we chose the [Fe_2O_3]-CaO and ZnO samples to study at lower temperatures. First, the [Fe_2O_3]CaO samples were studied at 250 °C and compared to the original ZnO samples. Table 4 shows the results obtained. It was found that [Fe_2O_3]-CP-CaO loses much of its reactivity at lower temperature, having a breakthrough number of 2 and saturation of 3. The [Fe_2O_3]AP-CaO sample, however, remained very reactive, having a breakthrough number of 10 and a saturation number of 23, which gives a molar ratio of (1 mol of H_2S):(3 mol of CaO); this is very close to the NC-ZnO molar ratio of (1 mol of H_2S):(2.4 mol of ZnO) (Figure 2).

The temperature was then decreased to 100 °C, and the results are shown in Table 5. With the temperature decrease, a significant loss in reactivity is seen with the CaO samples, but NC-ZnO still remains very active. Finally, the temperature was lowered to 25 °C. The

Table 4. Results from Low Temperature H_2S Studies

sample	temp (°C)	molar ratio
CM-1-ZnO	250	(1 mol of H_2S):(32 mol of ZnO)
CM-2-ZnO	250	(1 mol of H_2S):(5.8 mol of ZnO)
NC-ZnO	250	(1 mol of H_2S):(2.4 mol of ZnO)
[Fe_2O_3]CP-CaO	250	(1 mol of H_2S):(39 mol of CaO)
[Fe_2O_3]AP-CaO	250	(1 mol of H_2S):(3.0 mol of CaO)
CM-1-ZnO	100	(1 mol of H_2S):(38 mol of ZnO)
CM-2-ZnO	100	(1 mol of H_2S):(19 mol of ZnO)
NC-ZnO	100	(1 mol of H_2S):(3.5 mol of ZnO)
[Fe_2O_3]CP-CaO	100	(1 mol of H_2S):(39 mol of CaO)
[Fe_2O_3]AP-CaO	100	(1 mol of H_2S):(17 mol of CaO)
CM-1-ZnO	25	(1 mol of H_2S):(74 mol of ZnO)
CM-2-ZnO	25	(1 mol of H_2S):(52 mol of ZnO)
NC-ZnO	25	(1 mol of H_2S):(4.2 mol of ZnO)
[Fe_2O_3]CP-CaO	25	(1 mol of H_2S):(45 mol of CaO)
[Fe_2O_3]AP-CaO	25	(1 mol of H_2S):(45 mol of CaO)

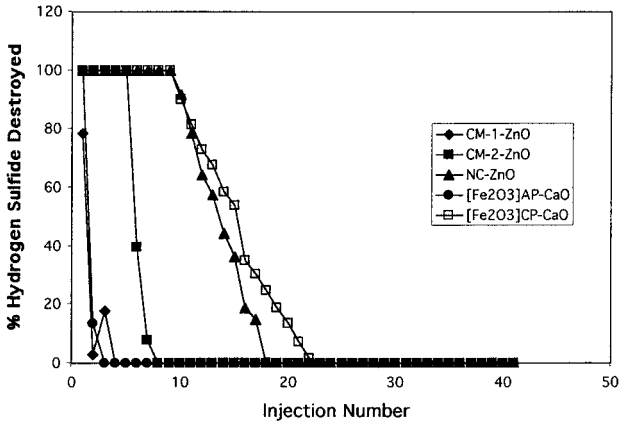

Figure 2. Percentage H_2S destroyed vs injection number at 250 °C for the ZnO and CaO samples.

Table 5. XRD Data after Reaction with H_2S

sample	2θ	assignment
CM-Al_2O_3	45.9, 67.1	Al_2O_3
NC-Al_2O_3	NA	
CM-MgO	37, 43, 62, 75, 79	MgO
CP-MgO	43, 62	MgO
AP-MgO	43, 62	MgO
[Fe_2O_3]AP-MgO	43, 62	MgO
[Fe_2O_3]CP-MgO	43, 62	MgO
CM-CaO	32, 37, 53, 64, 67, 79	CaO
	31, 45, 55, 65, 74	CaS
CP-CaO	37, 53	CaO
	33, 46, 50	CaS
AP-CaO	37, 53	CaO
	33, 46, 50	CaS
[Fe_2O_3]CP-CaO	37, 53, 67	CaO
	31, 45, 55, 65, 74	CaS
	50	Fe_2O_3
[Fe_2O_3]AP-CaO	37, 53	CaO
	31, 45, 55, 65, 74	CaS
CM-1-ZnO	32, 34, 36, 48, 57, 63, 66, 68, 69	ZnO
CM-2-ZnO	32, 34, 36, 48, 57, 63, 66, 68, 69	ZnO
NC-ZnO	32, 34, 36, 48	ZnO
	29, 48	ZnS

results are shown in Table 4 and clearly indicate that ZnO performs best.

(4) X-ray Diffraction. XRD was used to study the samples after reaction with H_2S. From Table 5, it can be seen that no spectral changes occur in the Al_2O_3 or MgO samples. This is somewhat expected as the reactivities of these samples were so low that a considerable amount of the oxide was not converted into the sulfide. However, in the cases of the calcium and zinc oxides, we do see the metal sulfide peaks present. In Figure 3 are the XRD spectra for CM-CaO, CP-CaO, and AP-CaO

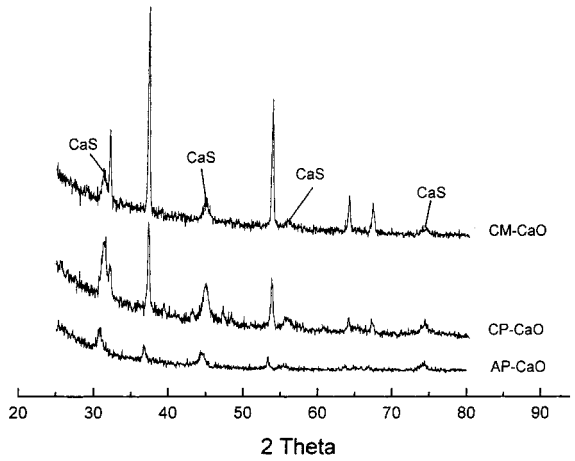

Figure 3. XRD spectra of CM-CaO, CP-CaO, and AP-CaO after reaction with H_2S at 500 °C.

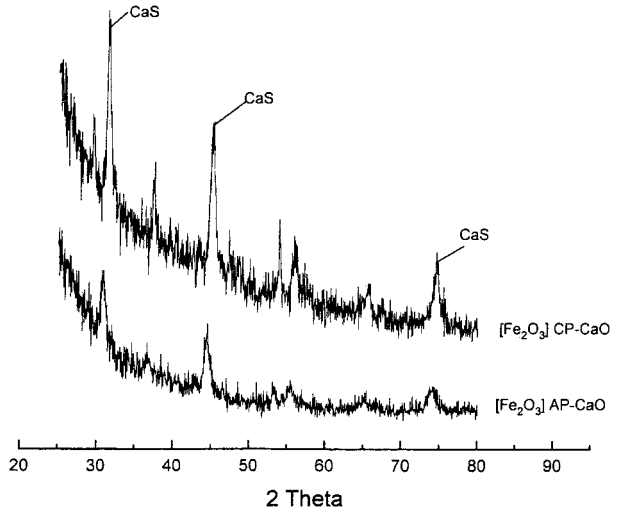

Figure 4. XRD spectra of [Fe_2O_3]AP-CaO and [Fe_2O_3]CP-CaO after reaction with H_2S at 500 °C.

after reaction with H_2S. In the spectra, the CaS peaks are identified, while all other peaks are due to CaO. Although the CM sample does show CaS peaks, in the CP and AP samples, the CaS peaks are the most dominant peaks present. Figure 4 shows the XRD spectra for the iron oxide-coated CaO samples. Here again, the CaS peaks are identified and are the most significant peaks present. The XRD spectra of the ZnO samples after reaction with H_2S are shown in Figure 5. No change can be seen in the spectra of the CM-1-ZnO and the CM-2-ZnO samples, whereas in the NC-ZnO spectrum, a new broad peak is in the position of the strongest ZnS peak.

Overall, it is clear that the NC samples are much more reactive than the CM samples. This increase in reactivity could be caused by several factors, including the increased surface area or possibly a change in morphology. To determine how the surface area affects this reaction, the percentage of metal oxide on the surface was mathematically determined. Table 6 shows the percentage of surface molecules using the indicated crystallite sizes. Next, the theoretical molar ratio was calculated, showing what the resulting molar ratio would be if a complete surface reaction occurred. By comparing this calculated molar ratio to the experimen-

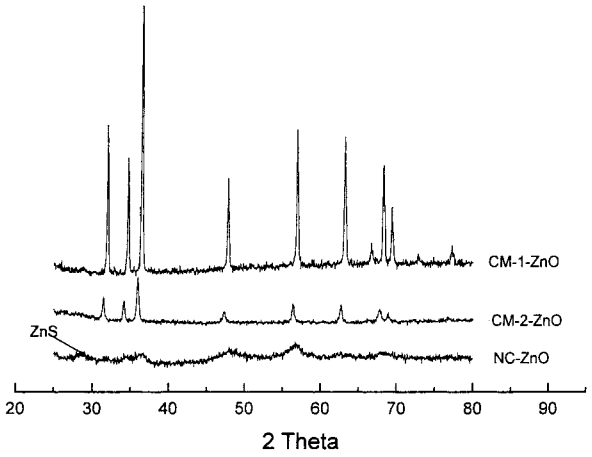

Figure 5. XRD spectra of CM-1-ZnO, CM-2-ZnO, and NC-ZnO after reaction with H_2S at 250 °C.

Table 6. Calculated Molar Ratio[a] Assuming Only Surface Reaction

sample	crystallite size (nm)	surface atoms (%)	molar ratio calc[b]	molar ratio exp[b]
NC-Al_2O_3	2	85	2.5:1	1:35
CM-Al_2O_3	19	4.7	1:7	1:340
CM-MgO	87	0.7	1:142	1:2700
CP-MgO	7	17	1:5.9	1:240
AP-MgO	4.5	27	1:3.7	1:190
[Fe_2O_3]CP-MgO	9	13	1:7.7	1:97
[Fe_2O_3]AP-MgO	6	20	1:5.0	1:70
CM-CaO	93	2.2	1:45	1:5.2
CP-CaO	15	13.5	1:7.4	1:2.6
AP-CaO	7	28	1:3.6	1:2.1
[Fe_2O_3]CP-CaO	16	12.6	1:7.9	1:1.7
[Fe_2O_3]AP-CaO	9	22.4	1:4.5	1:1.2
NC-ZnO	4	41.6	1:2.4	1:2.4
CM-1-ZnO	44	3.7	1:27	1:32
CM-2-ZnO	33	5.0	1:20	1:5.8

[a] Based on crystallite size. [b] Molar ratios in units of (mol of H_2S): (mol of oxide).

tal molar ratio, we can see that the increase in reactivity can be attributed to higher surface areas, although the least active oxides (Al_2O_3 and MgO) do not perform even as well as might be expected. However, in the case of the ZnO samples and essentially all of the CaO samples, higher surface areas (smaller crystallites) do have a beneficial effect. In addition, the reactions go deeper into the bulk, suggesting that crystal shape/morphology also plays a role. Indeed, the XRD data confirm that many layers are reacting to the extent that bulk stoichiometric processes take place.

IV. Discussion

For oxides for which the reaction with H_2S is thermodynamically unfavorable (MgO and Al_2O_3), the solid−gas reactions can be driven by temperature to a certain extent, and high surface areas and small crystallite sizes do help. However, not even full surface reactions can be obtained (see Table 6).

In the case of oxides for which the reaction is thermodynamically favored (ZnO and CaO), these solid−gas reactions can be driven very nearly to stoichiometric proportions. In these cases, higher surface areas and small crystallite sizes are also important, but crystal morphology must also play a role. In the cases of CP-CaO and AP-CaO, the reaction proceeds deep into the

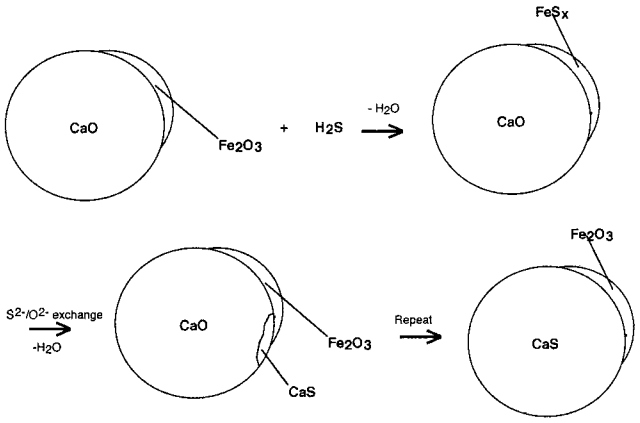

Figure 6. Proposed sequence for catalytic enhancement of H_2S adsorption.

nanocrystals, and this behavior is probably due to the existence of numerous edge/corner or defect sites or possible to crystal disorder, such that the H_2S penetration is facilitated[14−16].

In a similar vein, the presence of small amounts of surface Fe_2O_3 aids the H_2S reaction even further. This phenomenon has been observed before in the reaction of CCl_4 and sequestration of SO_2[7,13−14]

$$[Fe_2O_3]MgO + CCl_4 \rightarrow [Fe_2O_3]MgCl_2 + CO_2$$

$$[Fe_2O_3]CaO + SO_2 \rightarrow [Fe_2O_3]CaSO_4 + [Fe_2O_3]CaS$$

In this prior work, it was proposed that intermediate iron chlorides or iron sulfites were formed as mobile species that searched out reactive surface sites and then exchanged ions with the core MgO or CaO.[7,14] It is likely that a similar situation occurs with H_2S. Iron sulfides or oxysulfide surface species might form first and be mobile enough to seek out the more reactive sites or disordered sites on the nanocrystalline core oxide. This process could occur repeatedly, such that the Fe_2O_3 would serve as a catalyst driving these solid−gas reactions to stoichiometric proportions (see Figure 6). Thermodynamically, these reactions would be favorable, where iron sulfides or oxysulfides would be formed and would then carry the sulfide to surface sites where the sulfide could be exchanged with CaO in another energetically downhill reaction.

It is interesting to note that this type of catalysis has been observed in related systems with vanadium, manganese, and iron oxides. All contain metal ions capable of readily changing oxidation states, suggesting that this is feature important in the intimate mechanistic details (which are unknown at this time).[14]

As anticipated, the most efficient reaction takes place at higher temperature; for example, the [Fe_2O_3]AP-CaO-to-H_2S mole/mole ratio was 1.2 at 500 °C but 3.0 at 250 °C. For [Fe_2O_3]CP-CaO, this ratio was shifted from 1.2 to 39, clearly showing that the nanocrystalline AP samples were much more reactive at this lower temperature.

At 250 °C, ZnO proved to be the most active (see Table 6), particularly the nanocrystalline sample. At the lower temperatures (100 and 25 °C; see Table 4), efficiencies fell off, and the effect of Fe_2O_3 catalysis for CaO was not as pronounced. In these studies, the NC-ZnO sample clearly was superior.

It can be confidently concluded that, at elevated temperatures, nanocrystalline CaO and especially [Fe_2O_3]-CaO are the best choices for H_2S scrubbing, especially if the temperatures must be above 250 °C, where ZnO nanocrystals are unstable and sinter. If lower temperatures can be employed, especially 100 °C or lower, then ZnO appears to be superior.

Clearly kinetics are important as shown by (a) the enhancement in efficiency for smaller crystallites (higher surface area); (b) the fact that the smallest crystals are the most reactive on a surface area basis, presumably because of a preponderance of surface active sites and disorder; and (c) the observable catalytic effect of a transition metal oxide. Of course, thermodynamics also is a guiding force, as demonstrated by the relative inactivity of Al_2O_3 and MgO but high activities of ZnO and CaO.

Overall, it has been shown that nanoparticle metal oxides are preferred materials for hydrogen sulfide scrubbing. These materials are much more efficient than commercially available oxides for two major reasons. First, there is a much higher extent of reaction found with the nanoparticle metal oxides than with the commercial samples. For example, this is seen with the nanocrystalline zinc oxide, which reacts in a stoichiometric molar ratio of 1 mol of hydrogen sulfide to 2.4 mol of zinc oxide, whereas the commercial zinc oxide reacts in a molar ratio of 1 mol of hydrogen sulfide to 32 mol of zinc oxide. This difference in molar ratios could lead to 13 times less zinc oxide being used, as well 13 times fewer man hours to change out the bed, which allows for huge cost reductions. Second, another reason for the increased efficiency is that the nanoparticles are more active at lower temperatures. For example, nanocrystalline zinc oxide stays at a near-stoichiometric ratio at room temperature, whereas the commercial zinc oxide does not. This too is important for lowering processing costs.

Acknowledgment. The support of the National Science Foundation and the Army Research Office are acknowledged with gratitude.

CM011588R